ORIGINAL RESEARCH

Moisture absorption measurement and modelling of a cellulose acetate

S. Khoshtinat · **V. Carvelli** · **C. Marano**

Abstract With a view toward the application of highly hygroscopic polymers as a humidity responsive self-actuator, the evaluation of the real time moisture concentration in the material becomes a priority. In this paper, the moisture diffusion process in a cellulose acetate (53.3% of acetylation) has been studied. Membranes of cellulose acetate (thickness within the range 66–200 μm) have been prepared, and the moisture absorption at room temperature and at a different relative humidity (RH within the range 21–53%) has been monitored. An analytical model has been used to describe the observed non-Fickian sigmoidal behavior of moisture diffusion. A relaxation factor (β) of about 0.026 s^{-1} and a moisture diffusion coefficient (D) of 3.35×10^{-6} mm^2/s have been determined. At constant room temperature, the moisture concentration at saturation (C_{sat}) has shown a linear relation with relative humidity. The identified values β, D and C_{sat} of the analytical model have been used as input for the finite element simulation of the non-Fickian diffusion. The reliability of the finite element simulations has been confirmed with a second set of experiments.

Keywords Hygroscopic polymers · Non-Fickian moisture diffusion · Cellulose acetate · Finite element modeling

S. Khoshtinat · C. Marano (✉)
Department of Chemistry, Materials and Chemical Engineering "Giulio Natta", Politecnico Di Milano, Piazza Leonardo Da Vinci 32, 20133 Milan, Italy
e-mail: claudia.marano@polimi.it

S. Khoshtinat
e-mail: shiva.khoshtinat@polimi.it

V. Carvelli
Department of Architecture, Built Environment and Construction Engineering, Politecnico Di Milano, Piazza Leonardo Da Vinci 32, 20133 Milan, Italy
e-mail: valter.carvelli@polimi.it

Introduction

Hygroscopic materials are sensitive to changes in the environment humidity level. The moisture absorption can cause swelling, shrinkage, deformation, as well as a change in the rigidity of a hygroscopic material. Although the moisture absorption in polymers has often been considered as a disadvantage because it could affect the performance of a product during its service life (Xiaosong Ma et al. 2009; Wong 2010; Zhang et al. 2010), humidity sensitive polymers allow the manufacturing of sensors or actuators able to respond to a change in the environment humidity level (Ramirez-figueroa et al. 2016; Burgert and Fratzl 2009; Reyssat and Mahadevan 2009; Krieg et al. 2013;

Taccola et al. 2015; Yao et al. 2015; Menges and Reichert 2015; Holstov et al. 2015; Wang et al. 2016, 2017; Alexander and Korley 2017).

For a proper design of such devices the identification of constitutive models, describing the moisture absorption behavior of the material, is required. The Fickian solution of diffusion equation provides an analytical model with a constant diffusion coefficient. Studies on the diffusion mechanism in some polymers below their glass transition confirm a molecular relaxation due to the penetration of diffusive substances (Crank 1979). In this context, the Fickian law is not able to describe properly this phenomenon. In particular, highly hygroscopic materials experience a volumetric deformation during the moisture absorption process, which violates the boundary condition of the Fickian diffusion law (Crank and Park 1951; Crank 1953). Therefore, an analytical formulation that is able to describe this non-Fickian behavior with a constant diffusion coefficient becomes a priority for any simplified predictive model.

In glassy polymers, the absorbed moisture acts as a plasticizer, causing polymer relaxation and decreasing the glass transition temperature. Alfrey Jr et al. (1966) categorized diffusion in polymers as three different behaviors, Fickian, non-Fickian, and Case II, in relation to diffusion and polymer relaxation rates. Based on the same principles, Mensitieri and Scherillo (2011) classified the mass transport, which also describes the sorption ability of polymers. Depending on the hygroscopic material ability of water vapor sorption (uptake), we distinguish between: 'Moderate hygroscopic materials', which show a dual-stage sorption, with comparable rate of diffusion and relaxation and 'Highly hygroscopic materials', in which instead the diffusion rate is much higher than the relaxation rate, showing a sigmoidal trend in the absorption curve and a time dependent mass uptake.

Different approaches have been developed to describe the diffusion process of moisture-sensitive materials. In some studies the kinetic of the absorption and desorption processes has been assumed to be the same and the diffusion coefficient has been evaluated from desorption measurement and considered for the absorption process (Wong 2010). However, in highly hygroscopic materials that show a sigmoidal diffusion behavior, the kinetic of moisture absorption and desorption are completely different, as discussed by

Crank and Park (1951) and Mensitieri and Scherillo (2011).

Crank and Park (1951) investigated different anomalies of the diffusion and provided analytical models to interpret the experimental data. But these models cannot fully predict the experimental observations, as the diffusion can be influenced by the combination of different factors at the same time. In some glassy polymer, during the diffusion process, sharp boundaries between the glassy dried polymer and the polymer softened by vapor absorption can be observed through the thickness (Crank 1979). This is related to the combination of mechanical and physical effects of the diffusive substance on the membrane.

Cellulose-based materials, in this study cellulose acetate, are known for their hygroscopic behavior due to the presence of hydroxyl groups in their chemical structure (Chen et al. 2020; Lovikka et al. 2018). Cellulose acetate, which shows a sigmoidal behavior for moisture absorption, belongs to the highly hygroscopic material category (Mensitieri and Scherillo 2011). Roussis (1981) proposed a model with the rate of moisture induced molecular relaxation process that well fitted for membranes of cellulose acetate differing in thickness. De Wilde and Shopov (1994) proposed a simple model to describe a sigmoidal and a dual-stage diffusion, based on both Mensitieri and Scherillo (2011) classification and Cranks' theoretical investigations, by dividing the diffusion process in short-time and long-time phenomena. The *strain-dependent model* proposes a stepwise diffusion coefficient for the membrane changing from the rubbery to the glassy layer and defines the diffusion process as a function of time and concentration (Crank 1953, 1979). When the starting condition is the dry membrane (initial concentration $C_{initial} = 0$), the *strain-dependent model* can be simplified to the *variable surface concentration model* (Crank 1979).

In this study, a systematic characterization of the moisture absorption in cellulose acetate membranes has been performed evaluating the effect of membrane thickness and environment relative humidity level on the diffusion kinetic. Similar measurements for cellulose acetate have not been detailed in the literature, in the authors' knowledge. The kinetic of moisture absorption has been described using the variable surface concentration model. The material relaxation constant (β), the diffusion coefficient (D), and the concentration at saturation (C_{sat}), obtained by

experimental data best fitting, have been used as input parameters of finite element simulations to forecast the moisture diffusion through the thickness in other experimental conditions. The analytical and numerical models adopted in this study could be used for the real-time moisture concentration prediction of other cellulose-based materials or even for hydrogels. In particular, this study provides a robust methodology for the numerical modeling of the non-Fickian sigmoidal moisture diffusion behavior of hygroscopic materials by applying a simple time dependent surface concentration function.

Material, experimental measurements and analytical model

Cellulose Acetate (CA) powder (53.3% acetylation) was kindly provided by Mazzucchelli 1849 S.P.A. The Cellulose Acetate (CA) used in this study was made from cotton-based cellulose. Referring to literature (Rao and Diwan 1997; Al-Ahmed et al. 2004; Son et al. 2004; Heinze and Liebert 2004; Meier et al. 2004; Saljoughi et al. 2009; Zavastin et al. 2010; Medina-Gonzalez et al. 2011; Nolte et al. 2011), different approaches for cellulose acetate solution and membrane preparation have been investigated, considering different types of solvent, substrate, as well as different casting and solvent evaporation methods. A 20% w/w solution of Cellulose Acetate (CA) in ethyl lactate ($\geq$ 98% purity, purchased from Sigma-Aldrich) was prepared by gradually adding the CA powder to the solvent. Mixing was performed at 80 °C using RCT basic IKAMAG^{TM} safety control magnetic stirrer. The solution was kept under stirring at $300 rpm$ for 90 minutes and then at 200 rpm for further 90 min. It was then left to cool down and reach the room temperature overnight.

The solution was poured on a glass substrate, at room temperature, and a film of about 500 μm thickness was casted by K Control Coater at the lowest velocity (3 mm/s) to avoid any process-induced orientation of polymer molecules. Drying of CA film was carried out in two steps at room temperature. First, the membrane was kept in a close chamber, without air flow, for 3 h to reduce solvent evaporation at the beginning of the drying process to avoid bubbles formation. Then, it was dried for 4 h in Vuototest Mazzali vacuum oven to fast complete the

solvent evaporation. With this procedure, membranes of thicknesses ranging from 66 ± 1.5 to 70 ± 4.5 μm were obtained. Thicker membranes with thicknesses between 145 ± 2 and 200.0 ± 10.5 μm have been obtained performing the described procedure twice, using a dried CA membrane as the substrate in the second step, instead of glass. Square samples of 30×30 mm^2 were then punched from the obtained membranes.

Although the standard procedure for moisture content measurement of un-plasticized cellulose acetate (BS EN ISO 585:1999) suggests to dry cellulose acetate (independently of its physical form) for 3 h at 105 °C, drying has not been completed after even 6 h in the suggested conditions. Therefore, each specimen was dried at 125 °C for 24 h in oven (Mazzali Thermair), then placed and kept for 2 h in a desiccator at room temperature. All the gravimetric measurements were performed by an AS310.R2 (RADWAG) balance, with a resolution of 0.1 mg, in a climatized room at 25 ± 1 °C, at a constant value of relative humidity (RH within the range 21–53%). Although the climatized room has homogeneous air conditioning without any direct airflow, the side doors of the balance shield were kept closed during the test to prevent any further airflow effect. The top door of the balance shield was instead kept open to ensure the humidity of the balance shield to be equal to that of the climatized room. The dried specimens were put directly at the center of the balance weighing pan to avoid the possible error due to the effect of the sample holder's weight. Since the specimens obtained by membrane punching were not plane, the curvature of the specimen allowed it to be positioned on the balance pan in such a way that the membrane could absorb moisture equally from both the main surfaces. Experimental data repeatability is a confirmation of the homogeneous absorption conditions for all the specimens, irrespective of their different curvature (see Fig. 1a). Finally, the moisture absorption process of the dried cellulose acetate membranes was monitored at different values of RH, measuring the moisture mass variation in time.

For the sake of brevity, Fig. 1 reports only some of the obtained experimental results, to demonstrate the repeatability and elucidate the effect of thickness and relative humidity. The rest of the experimental results are reported in Online Resource 1. Figure 1a shows the experimental data of the moisture absorption in
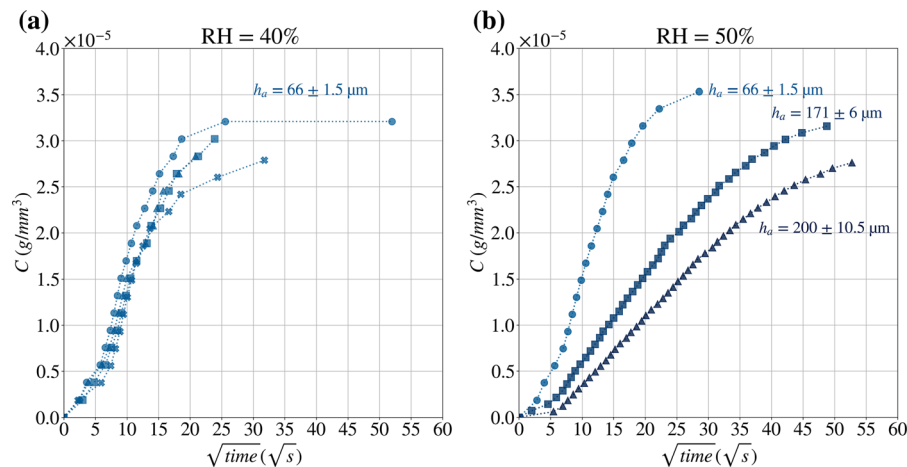
Fig. 1 Moisture absorption in cellulose acetate membranes: **a** Moisture absorption repeatability at 40% of relative humidity for a membrane with thickness $h_a = 66 \pm 1.5$ μm; **b** moisture absorption at 50% of relative humidity for different thickness of the membrane

two specimens with a thickness of 66 ± 1.5 μm, for a relative humidity of 40%, which was repeated twice for each specimen. From the theoretical point of view, the time needed for a sample to reach its saturation concentration is a function of the sample thickness. Thinner membranes reach concentration at saturation sooner than thicker membranes (Wong 2010). For this reason, the duration of the absorption measurements was not the same for the different thick specimens. In this study, the absorption process was assumed to be completed when moisture uptake was slower than $10^{-9} \frac{g}{mm^3 \cdot s}$.

A sigmoidal trend is evident in all the curves. The rate of absorption is small during the initial 50 s ($\sqrt{time} \approx 7$) of exposure of the dried membrane and then a fast increase in the rate of absorption can be observed. A sigmoidal trend can be still observed at a higher level of humidity (RH = 50%), for the same thickness ($h_a = 66 \pm 1.5$ μm), and for higher thicknesses ($h_a = 171 \pm 6$ and 200 ± 10.5 μm)(Fig. 1b).

By comparing the results for the membrane with thickness 66 ± 1.5 μm in Fig. 1a and b, it can be observed that moisture uptake is not affected by the environment humidity at least for an exposure time up to about 225 s ($\sqrt{time} \approx 15$). As expected, for longer exposure times, the higher the relative humidity, the higher the moisture absorbed, as well its asymptotic value at saturation (C_{sat}). At the relative humidity of 40%, C_{sat} is 3.2×10^{-5} g/mm³ and it takes about 650 s ($\sqrt{time} \approx 25$) to reach this value, while at the relative humidity of 50%, the concentration at

saturation is of 3.5×10^{-5} g/mm³. Moreover, Fig. 1b points out that, for any exposure time before saturation (see e.g. t $\approx$ 100 s, $\sqrt{time} \approx 10$), the lower the membrane thickness the higher the moisture concentration, as expected.

When a material shows a Fickian behavior, the diffusion coefficient is estimated by a linear fitting of the data reproducing the ratio M_t/M_∞ as function of the square root of the absorption time ($\sqrt{time}$) up to $\frac{M_t}{M_\infty} < 0.5$, using a simplified version of the Fickian behavior formula $\left(\frac{C_t}{C_\infty} = \frac{M_t}{M_\infty} = 4\sqrt{\frac{D \cdot t}{\pi h^2}}, C = \frac{M}{V} \right)$, where, M_t and M_∞ are the moisture mass at time t and at saturation, respectively (Wong 2010). For the material considered in the present study, this approach cannot be applied to the experimental data in Fig. 1, because the absorption curve slope changes at least four orders of magnitude before $\sqrt{time} < 7$ and after $\sqrt{time} > 7$. This indicates, the coefficient of diffusion is a function of time and moisture concentration. Therefore, the general solution of Fickian equation is not suitable for this material. The diffusion anomaly derives from the peculiar hygroscopic behavior of cellulose-based materials. Water molecules create hydrogen bonds with hydroxyl groups and disturb the interchain interaction in the polymer, acting as polymer plasticizers (Wong 2010) and thus decreasing its glass transition temperature and reducing its rigidity. Due to the increase of molecular mobility at the surface of the membrane, the polymer mechanical properties are different through the membrane

thickness. The expansion in the surface layer induces an internal stress between the rubbery surface and the dry glassy core of the membrane (De Wilde and Shopov 1994). The relaxation caused by moisture absorption on the surface layer and the time needed for stabilization of the polymer molecules are responsible of the delay in the diffusion process, and can explain the observed non-linear trend in the moisture absorption curves (Crank and Park 1951; Crank 1979; De Wilde and Shopov 1994).

As suggested in literature (Crank and Park 1951; Crank 1953, 1979), assuming for the surface layer the same law of diffusion but with a different relaxation time, the surface layer reaches its saturation concentration exponentially according to Eq. 1, where C_t and C_{sat} are the concentration at time t and at saturation respectively and β is the relaxation factor.

$$C_t = C_{sat}\left(1 - e^{-\beta t}\right) \tag{1}$$

Therefore, we can define a diffusion coefficient dependent only on concentration, while considering the violated boundary conditions of the general diffusion laws in terms of the relaxation factor (β). For the specific initial condition of a completely dried membrane ($C_0 = 0$), the analytical model known as the "*variable surface concentration model*", detailed in Eq. 2, is here considered (Crank and Park 1951; Crank 1953, 1979).

$$\frac{M_t}{2lC_{Sat}} = 1 - e^{-\beta t}\cdot\sqrt{\frac{D}{\beta l^2}}\cdot\tan\left(\sqrt{\frac{\beta l^2}{D}}\right)$$
$$- \sum_{n=0}^{\infty}\frac{8}{\pi^2}\cdot\frac{\exp\left(-\frac{(2n+1)^2\pi^2 Dt}{4l^2}\right)}{(2n+1)^2\left\{1 - (2n+1)^2\left(\frac{D\pi^2}{4\beta l^2}\right)\right\}} \tag{2}$$

M_t is the moisture mass absorbed per unit area by the membrane at time t, l is half-thickness of the membrane ($l = h_a/2$), D is the constant diffusion coefficient and β is the relaxation constant $\left(\beta \neq (2n+1)^2\left(\frac{D\pi^2}{4l^2}\right)\right)$. A parametric study on the effect of C_{sat}, D, β for this analytical model (Eq. 2) has been presented in Online Resource 2. From the best fitting of the gravimetric experimental data with Eq. 2, by the least squared method, the parameters C_{sat}, D, β were obtained. The accuracy of the fitted model has been evaluated by *R-scored* method. The best fitting of all the experimental data (different relative humidity

and membrane thickness) provided the optimized parameters β, D, C_{sat} with $R^2 > 0.95$, which are detailed in Figs. 2, 3, 4.

Figure 2 shows, as an example, the evolution of moisture concentration versus the square root of time for the specimens presented in Fig. 1b, exposed to 50% of relative humidity, together with the analytical model prediction. At the first glance, the analytical model well describes the sigmoidal trend of absorption curve, and it can well predict the behavior for time ranges wider than the reasonable short explored ones. By the way, in the very early stage of the absorption process ($\sqrt{time} = 5 \sqrt{s}$), a slight disagreement between the analytical model and the experimental data can be observed for the membrane with the thickness of 66 ± 1.5 μm. The accurate fitting by Eq. 2 can estimate several features, namely: the time at the sigmoidal curve inflection point, the concentration at saturation and the slope of the long-time sorption phase (linear part). It must be pointed out that the predicted value of D is not the slope of neither early stage of absorption nor the middle stage of absorption.

Figure 3 shows the values of moisture concentration at saturation (C_{sat}), obtained by experimental data extrapolation with the analytical model, as a function of relative humidity: the average values and the relevant standard deviation are reported. Since, at a constant temperature, the water partial vapor pressure at saturation (p_{sat}) and the water vapor solubility (S) are independent of relative humidity, the moisture concentration at saturation (C_{sat}) has a linear relation with relative humidity as ($C_{sat} = (S \times p_{sat}) \times RH$) (Fan et al. 2009; Wong 2010). Hypothetically, in a dry environment (RH = 0%), the moisture concentration at saturation is zero ($C_{sat} = 0$). Therefore, by applying a linear fit to the experimental data, which passes also through the origin (see Fig. 3) the linear function $C_{sat} = 6.91 \times 10^{-7} \times RH$ is obtained with a correlation coefficient of $R^2 = 0.982$. This equation allows to predict the moisture concentration at saturation in the considered material at a constant temperature and at vary relative humidity.

Figure 4 reports the material properties D and β obtained from the best fitting of experimental data to the analytical model for each moisture absorption. The values of the diffusion coefficient (D) varied from 2.97×10^{-6} to 4.18×10^{-6} mm²/s, with a mean value
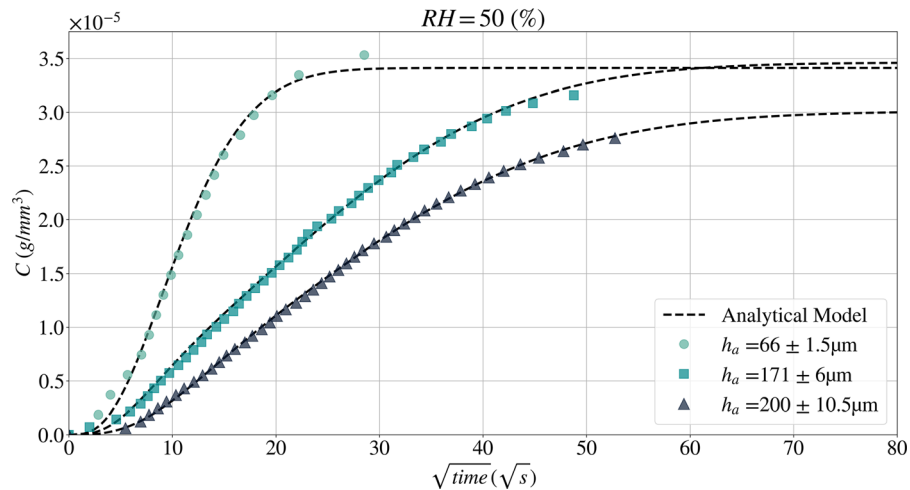
Fig. 2 Analytical model prediction and experimental data of moisture absorption in membranes of different thickness at RH = 50%
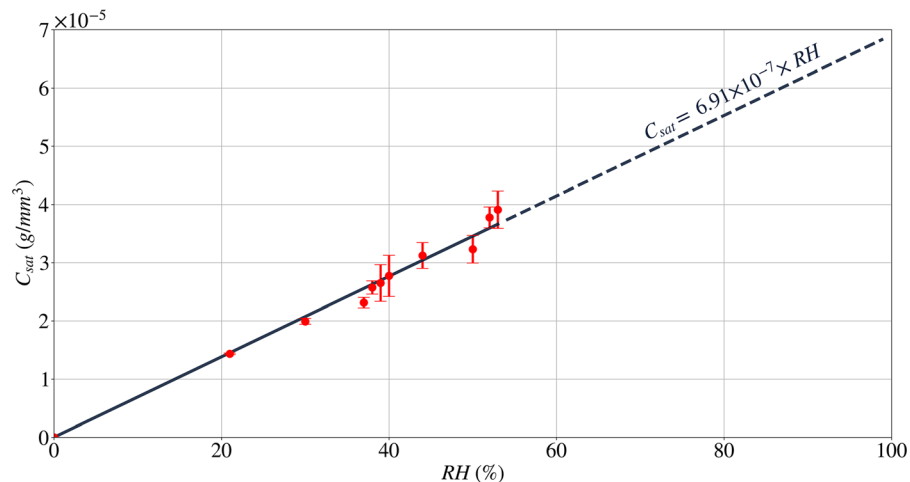

Fig. 3 Average moisture concentration at saturation as a function of environment relative humidity (bars represent standard deviation of the experimental data) and linear interpolation (continuous line)

of 3.35×10^{-6} and the relevant standard deviation of 3.02×10^{-7} (Fig. 4a). Figure 4b shows the values for β in the range between 0.001 and 0.046 s^{-1} with a mean value of 0.026 s^{-1} and the standard deviation of 0.013.

Comparing the two graphs from a qualitative point of view, it can be observed that the obtained values for the diffusion coefficient (D) are in a narrower experimental band compared to the relaxation factor (β). For the dispersion of the relaxation factor (β) no trend can been observed, neither with respect to the thickness nor to the relative humidity. However, considering the negligible effect of a variation of the

relaxation factor (β) between 0.01 and 0.1 s^{-1} on the predicted absorption curve, as shown in the Online Resource 2 (c), the use of β mean value as input of the numerical model described in the next section, should not cause inaccurate predictions.

Finite element modelling

Finite element simulations were performed by COM-SOL Multiphysics® 5.6. A 3D prismatic geometry has been used to discretize three samples with dimensions of $1 \times 1 \times$ thickness (mm³) at two different values of

(a)

(b)

▲ $h_a = 66 \pm 1.5\ \mu m$　　● $h_a = 161 \pm 7\ \mu m$　　✖ $h_a = 171 \pm 6\ \mu m$　　■ $h_a = 200 \pm 10.5\ \mu m$
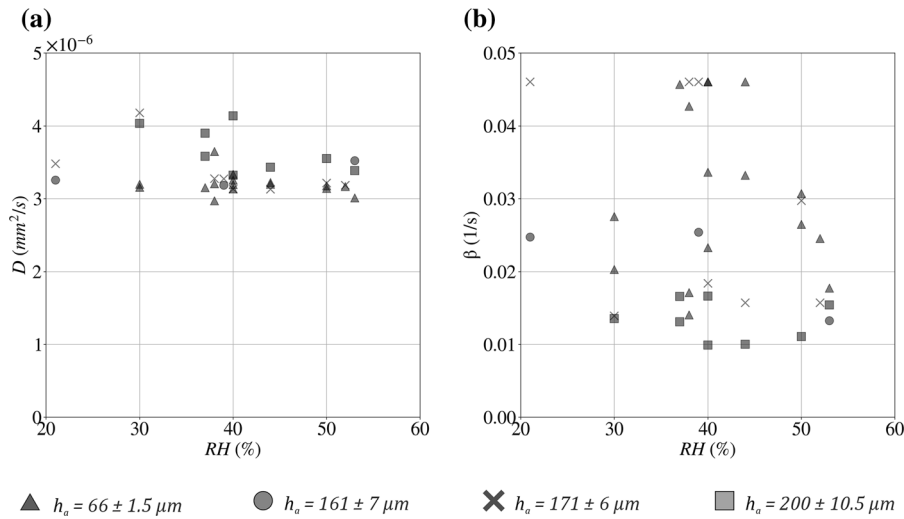
Fig. 4 Values of **a** diffusion coefficient, D, and **b** relaxation constant, β, obtained by the best fitting of experimental data of moisture absorption tests, performed at different values of relative humidity, RH, using several specimens differing in their thickness, h_a

relative humidity, see Fig. 5a. The time dependent model "Transport of Diluted Species" from chemical transport interface has been used, which is based on Fick's law. The convection transport mechanism with linear discretization of concentration has been used for the simulations. To the best of the authors' knowledge, the code is not able to simulate sigmoidal non-Fickian behavior directly. Therefore, in the global definition the values of β (s^{-1}), D (mm^2/s) and C_{sat} (g/mm^2) obtained fitting the experimental results by the analytical model have been used as inputs. The no flux boundary condition has been applied to the four

surfaces of membrane thickness. Since the experimental procedure was dedicated to a completely dry membrane, the initial value of moisture concentration in the membrane, C_{sat}, was set equal to zero.

The concentration was applied as boundary condition on two lateral surfaces of the membrane (Fig. 5). As mentioned, the delay in the diffusion process (sigmoidal behavior) is caused by the surface layer, which gets its final concentration according to the function $C_t = C_{sat}\left(1 - e^{-\beta t}\right)$. Therefore, instead of a constant boundary condition with the value of C_{sat} (Fickian behavior), Eq. 1 has been adopted for the
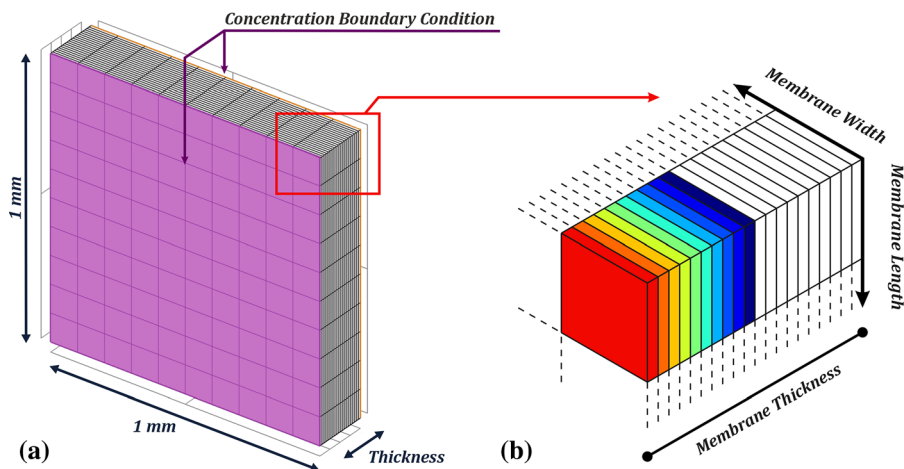

Fig. 5 Details of finite element model. **a** Sample dimensions, boundary conditions and discretization, **b** elements set to monitor the concentration at each time increment

concentration by recalling the mentioned parameters defined in the global definition.

A user-controlled, general physics swept mesh with quadrilateral face through a straight-line path has been applied from one lateral surface to the other, which generates a discretized volume by hexahedral elements. This approach provided an adequate distribution of elements, 20 elements along the thickness and 10×10 elements on the surface 1×1 mm^2 (total of 2000 elements), while reducing the computational time.

From the experimental measurements it was found that the thickest sample reached the moisture concentration at saturation after about 90 min (5400 s); hence, a time increment of 2 s was chosen to simulate the diffusion process up to 6400 s. For a better understanding of the evolution of concentration in time along the thickness, which is not straightforward (or possible) to measure experimentally, the concentration at each time increment was extracted for the elements set in Fig. 5b. The average concentration in volume for each time increment was estimated as function of the square root of time.

A preliminary insight in the numerical model accuracy is on the influence of the considered exponential function for the diffusion process through the thickness compared to the general Fickian behavior. The sample with a thickness of 200 μm at the relative humidity of 50% was simulated with the mean values of β, D and C$_{sat}$ in Table 1. As mentioned, twenty elements have been used through the specimen thickness. Since moisture diffusion is symmetrical with respect to the midplane (see Fig. 5), ten elements have been considered for detailing the results (colored elements in Fig. 5b).

Figure 6 depicts the evolution of concentration versus thickness for a Fickian and non-Fickian diffusion by the initial 100 seconds, each curve represents a time interval of 5 s. In the Fickian behavior simulation (Fig. 6a), since the beginning of the moisture absorption process (t = 0 s), the surface element instantaneously reached a concentration of 3.45×10^{-5} g/mm^3. So, the moisture diffuses through the thickness starting from this value of concentration at saturation. For the non-Fickian behavior simulation (Fig. 6b), at t = 0 s, the concentration is zero. As can be seen, even after 100 s, the surface element still doesn't reach its concentration at saturation. This delay influences the whole process of moisture absorption and generates the initial gradual variation of the slope of the sigmoidal curve observed experimentally (Fig. 2).

Results and discussion

The effect of the input parameters (β, D and C$_{sat}$) has been studied by modelling the samples presented in Fig. 2 with two sets of values (see Table 1). Set 1 consists of the values obtained from the fitting procedure carried out for the experimental data of each membrane thickness in Table 1. Set 2 consists of the mean values for β and D (Table 1) evaluated considering all the experiments (see Fig. 4a and b). For both sets, C$_{sat}$ of 3.45×10^{-5} g/mm^3 was obtained from Fig. 3 at the relative humidity of 50%. Figure 7 reports the FEM predicted moisture concentration versus square root of time for the two sets of mentioned input values, compared to the experimental data. The FEM simulations with input from each membrane thickness almost overlap the experimental data. Simulations with the mean values provide some interesting insight about each optimized value and their effect on the trend of the curves. Therefore, here we just compared the two simulations results. Regarding the trend of the curve in the very early stage of moisture absorption, which is mainly governed by the relaxation factor (β), the two simulations are in a good agreement, as expected for the membranes with the thickness of 66 and 171 μm, having β very close to the mean value, see Table 1. The negligible difference between the two simulations for the membrane with

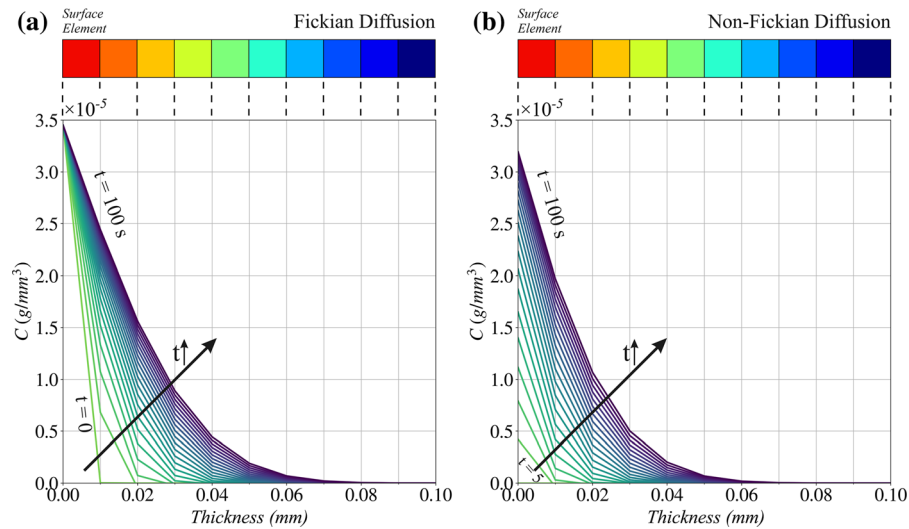|	RH (%)	h$_a$ (mm)	β (1/s)	D (mm^2/s)	C$_{sat}$ (g/mm^3)
Table 1 Input of finite element simulation	50	0.066	0.026	3.14×10^{-06}	3.41×10^{-05}
		0.171	0.030	3.22×10^{-06}	3.46×10^{-05}
		0.2	0.011	3.55×10^{-06}	3.01×10^{-05}
		Mean Values	0.026	3.35×10^{-06}	3.45×10^{-05}

Fig. 6 Comparison between simulation of moisture diffusion through thickness with **a** Fickian and **b** non-Fickian behavior
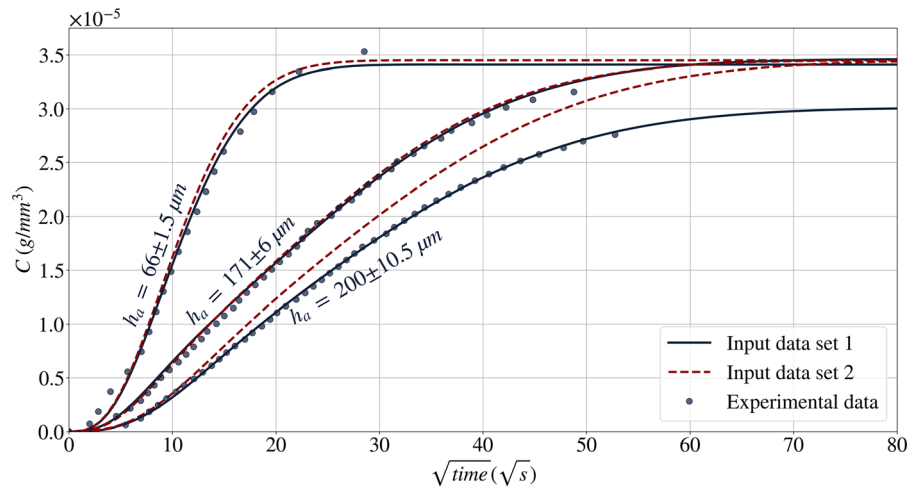

Fig. 7 Comparison between experimental data and finite element simulations

the thickness of 200 μm ($\beta = 0.011$ s^{-1}) in this stage confirms that the variation of β in Fig. 4b does not affect considerably the model.

Instead, the late stage of moisture absorption is mostly affected by two parameters: diffusion coefficient (D) and concentration at saturation (C$_{sat}$). The two simulation curves for the membrane with the thickness of 171 μm, which had the closest values of D and C$_{sat}$ to the mean values, almost overlap each other through the whole process of absorption. For the thinnest membrane (h$_a$ = 66 ± 1.5 μm), the prediction capability of the FEM simulation with mean values remains very high. Due to the relatively higher

mean diffusion coefficient with respect to the one proper to that thickness, a slight shift to the left in this stage can be observed.

The results of the simulations for the thickest specimen (h$_a$ = 200 ± 10.5 μm) highlight which property, C$_{sat}$ or D, determines the trend of the absorption curve. For this membrane (Table 1), the mean diffusion coefficient has a lower value compared to the one proper to that thickness. According to the parametric study in Online Resource 2 (d), the decrease in diffusion coefficient should shift the curve to the right. It is visible for the simulation with the mean diffusion coefficient which shifts to the left the

prediction. This huge shift in the opposite direction, indeed, is governed by the higher level of concentration at saturation (C_{sat}).

To explore the reliability of the finite element model, another set of experiments was carried out and the results compared to the predictions. Two membranes with thicknesses of $h_a = 70.5 \pm 3$ and 145 ± 2 µm, different than presented above, have been prepared and characterized. The specimens were also weighted after 90 min of exposure to corresponding values of the relative humidity. Since the number of experimental data points for thin membranes ($h_a < 100$ µm) is almost half of the experimental data points for thicker membranes ($h_a > 100$ µm), the experiments were repeated twice for the membrane with thickness of 70.5 ± 3 µm. Figure 8 details the moisture absorption experiment results for this new set of membranes together with their finite element simulations.. It must be noticed that, as expect, the average values of the concentration at saturation at each value of relative humidity for this set of membranes are consistent with the data reported in Fig. 3. For each of the two thicknesses, three simulations were performed, for a different value of relative humidity (RH = 20, 38, 52%). The values of β and D reported in Table 1 were used as input of these membrane simulations. The C_{sat} was instead calculated by the linear function between C_{sat} and relative humidity in Fig. 3.

It can be stated that the predictions of finite element simulation are in good agreement with experimental data ($R^2 > 0.98$), which highlights the accuracy of the numerical model for the behavior of membranes with different thickness than the ones adopted to estimate the input parameters.

Conclusions

Moisture absorption of dried cellulose acetate membranes was monitored experimentally at a constant temperature (25 ± 1 °C) and for different levels of relative humidity (RH within the range 21–53%): a sigmoidal behavior has been always observed. The analytical model known as variable surface concentration has been used to describe this non-Fickian moisture diffusion behavior. This model provides a value of diffusion coefficient (D) which is constant during the whole process of moisture absorption, by considering the polymer relaxation. The material properties β, D, and the moisture concentration at saturation, C_{sat}, have been obtained by fitting the experimental data with the analytical model. Moreover, the linear relationship between relative humidity and concentration at saturation has been estimated as $C_{sat} = 6.91 \times 10^{-7} \times RH$.

The finite element simulation for non-Fickian diffusion has been performed by COMSOL Multiphysics® 5.6, considering the concentration as an exponential function of relaxation factor (β) and moisture concentration at saturation (C_{sat}). The simulations were performed for three specimens at a constant relative humidity, once with the values retrieved from the fitting of the analytical model and
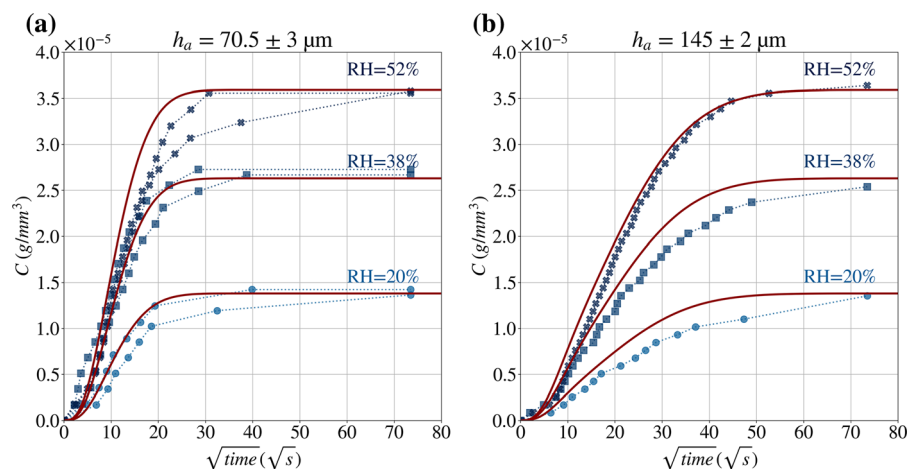

Fig. 8 Comparison between experimental moisture absorption (dotted lines and symbols) and FEM prediction (continuous lines)

another with the mean values of β, D, and C_{sat}, calculated from all the experimental data. The comparison between the FE simulation and the experimental data showed a considerable good agreement and confirmed the validity of the simulation procedure.

This numerical model provides a more in depth understanding and description, than experimental measurements, of the sigmoidal behavior showed by the studied cellulose acetate at different values of relative humidity. Further steps of the study will consider the effect of temperature on the parameters β, D and C_{sat}, as well the degree of acetylation of the cellulose.

Code availability Software application or custom code are available on request.

Data availability All the data has been reported as *Online Resource.*

Declarations

Conflict of interest The authors declare that they have no known competing financial interests or personal relationships that could have appeared to influence the work reported in this paper.

Consent to participate All authors gave explicit consent to participate.

Consent for publication All authors gave explicit consent to submit.

References

Al-Ahmed A, Mohammad F, Ab Z, Rahman M (2004) Composites of polyaniline and cellulose acetate: preparation, characterization, thermo-oxidative degradation and stability in terms of DC electrical conductivity retention. Synth Met 144:29–49. https://doi.org/10.1016/j.synthmet.2004.01.007

Alexander SLM, Korley LTJ (2017) Tunable hygromorphism: structural implications of low molecular weight gels and electrospun nanofibers in bilayer composites. Soft Matter 13:283–291. https://doi.org/10.1039/C6SM00749J

Alfrey T Jr, Gurnee EF, Lloyd WG (1966) Diffusion in glassy polymers. J Polym Sci Part C: Polym Symp 12:249–261. https://doi.org/10.1002/polc.5070120119

Burgert I, Fratzl P (2009) Actuation systems in plants as prototypes for bioinspired devices. Philos Trans R Soc A Math Phys Eng Sci 367:1541–1557. https://doi.org/10.1098/rsta.2009.0003

Chen Q, Fang C, Wang G et al (2020) Hygroscopic swelling of moso bamboo cells. Cellulose 27:611–620. https://doi.org/10.1007/s10570-019-02833-y

Crank J (1953) A theoretical investigation of the influence of molecular relaxation and internal stress on diffusion in polymers. J Polym Sci 11:151–168. https://doi.org/10.1002/pol.1953.120110206

Crank J (1979) The mathematics of diffusion. Oxford University Press

Crank J, Park GS (1951) Diffusion in high polymers: some anomalies and their significance. Trans Faraday Soc 47:1072. https://doi.org/10.1039/tf9514701072

De Wilde WP, Shopov PJ (1994) A simple model for moisture sorption in epoxies with sigmoidal and two-stage sorption effects. Compos Struct 27:243–252. https://doi.org/10.1016/0263-8223(94)90085-X

Fan XJ, Lee SWR, Han Q (2009) Experimental investigations and model study of moisture behaviors in polymeric materials. Microelectron Reliab 49:861–871. https://doi.org/10.1016/j.microrel.2009.03.006

Heinze T, Liebert T (2004) 4.2 Chemical characteristics of cellulose acetate. Macromol Symp 208:167–238. https://doi.org/10.1002/masy.200450408

Holstov A, Bridgens B, Farmer G (2015) Hygromorphic materials for sustainable responsive architecture. Constr Build Mater 98:570–582. https://doi.org/10.1016/j.conbuildmat.2015.08.136

Krieg O, Christian Z, Correa D, et al (2013) HygroSkin–meteorosensitive pavilion

Lovikka VA, Rautkari I, Maloney TC (2018) Changes in the hygroscopic behavior of cellulose due to variations in relative humidity. Cellulose 25:87–104. https://doi.org/10.1007/s10570-017-1570-9

Medina-Gonzalez Y, Aimar P, Lahitte J-F, Remigy J-C (2011) Towards green membranes: preparation of cellulose

acetate ultrafiltration membranes using methyl lactate as a biosolvent. Int J Sustain Eng 4:75–83. https://doi.org/10.1080/19397038.2010.497230

Meier MM, Kanis LA, de Lima JC et al (2004) Poly(caprolactone triol) as plasticizer agent for cellulose acetate films: influence of the preparation procedure and plasticizer content on the physico-chemical properties. Polym Adv Technol 15:593–600. https://doi.org/10.1002/pat.517

Menges A, Reichert S (2015) Performative wood: physically programming the responsive architecture of the hygroscope and hygroskin projects. Archit Des 85:66–73. https://doi.org/10.1002/ad.1956

Mensitieri G, Scherillo G (2012) Environmental resistance of high performance polymeric matrices andcomposites. In: Wiley encyclopedia of composites. Wiley Inc., Hoboken, NJ, USA. https://doi.org/10.1002/9781118097298.weoc074

Nolte MCM, Simon PFW, del Toro MA et al (2011) Cellulose acetate reverse osmosis membranes made by phase inversion method: effects of a shear treatment applied to the casting solution on the membrane structure and performance. Sep Sci Technol 46:395–403. https://doi.org/10.1080/01496395.2010.521231

Ramirez-figueroa C, Hernan L, Guyet A, Dade-robertson M (2016) Bacterial hygromorphs: experiments into the integration of soft technologies into building skins. In: Proceedings of the 36th annual conference of the Association for Computer Aided Design in Architecture (ACADIA), 27 Oct 2016–29 Oct 2019, Ann Arbor, MI, USA, pp 244–253. ISBN 978-0-692-77095-5

Rao PR, Diwan PV (1997) Permeability studies of cellulose acetate free films for transdermal use: influence of plasticizers. Pharm Acta Helv 72:47–51. https://doi.org/10.1016/S0031-6865(96)00060-X

Reyssat E, Mahadevan L (2009) Hygromorphs: from pine cones to biomimetic bilayers. J R Soc Interface 6:951–957. https://doi.org/10.1098/rsif.2009.0184

Roussis PP (1981) Diffusion of water vapour in cellulose acetate: 1. differential transient sorption kinetics and equilibria. Polymer (guildf) 22:768–773. https://doi.org/10.1016/0032-3861(81)90012-4

Saljoughi E, Sadrzadeh M, Mohammadi T (2009) Effect of preparation variables on morphology and pure water permeation flux through asymmetric cellulose acetate membranes. J Memb Sci 326:627–634. https://doi.org/10.1016/j.memsci.2008.10.044

Son WK, Youk JH, Lee TS, Park WH (2004) Preparation of antimicrobial ultrafine cellulose acetate fibers with silver nanoparticles. Macromol Rapid Commun 25:1632–1637. https://doi.org/10.1002/marc.200400323

Taccola S, Greco F, Sinibaldi E et al (2015) Toward a new generation of electrically controllable hygromorphic soft actuators. Adv Mater 27:1668–1675. https://doi.org/10.1002/adma.201404772

Wang DH, McKenzie RN, Buskohl PR et al (2016) Hygromorphic polymers: synthesis, retro-michael reaction, and humidity-driven actuation of ester-sulfonyl polyimides and thermally derived copolyimides. Macromolecules 49:3286–3299. https://doi.org/10.1021/acs.macromol.6b00250

Wang W, Yao L, Cheng C-Y et al (2017) Harnessing the hygroscopic and biofluorescent behaviors of genetically tractable microbial cells to design biohybrid wearables. Sci Adv 3:e1601984. https://doi.org/10.1126/sciadv.1601984

Wong CP (2010) Moisture sensitivity of plastic packages of IC devices. Springer, US, Boston, MA

Xiaosong Ma, Jansen KMB, Ernst LJ, et al (2009) A new method to measure the moisture expansion in plastic packaging materials. In: 2009 59th Electronic Components and Technology Conference. IEEE, pp 1271–1276

Yao L, Ou J, Cheng C-Y, et al (2015) bioLogic. In: Proceedings of the 33rd Annual ACM Conference on Human Factors in Computing Systems. ACM, New York, NY, USA, pp 1–10

Zavastin D, Cretescu I, Bezdadea M et al (2010) Preparation, characterization and applicability of cellulose acetate–polyurethane blend membrane in separation techniques. Colloids Surfaces A Physicochem Eng Asp 370:120–128. https://doi.org/10.1016/j.colsurfa.2010.08.058

Zhang H, Park S, Hong S (2010) Hygroscopic swelling behavior of molding compound at high temperature. In: 2010 12th IEEE Intersociety Conference on Thermal and Thermomechanical Phenomena in Electronic Systems. IEEE, pp 1–7